NASA DEVELOP National Program
Virginia – Langley

Spring 2020

Toa Baja Disasters

Utilizing Open-Source Earth Observations to Inform the Toa Baja Municipality's Flood Mitigation Efforts and Educate the Public

DEVELOP Technical Report
Final Draft – April 2nd, 2020

Nara McCray (Project Lead)
Scott Harrison
Wilfredo A. Garcia Lopez
Adriana S. Le Compte Santiago

Dr. Kenton Ross, NASA Langley Research Center (Science Advisor)
Dr. Venkataraman Lakshmi, University of Virginia Department of Engineering Systems and the Environment (Science Advisor)

1. Abstract

Toa Baja, located just west of San Juan in Puerto Rico, is known as "the underwater city" due to its propensity to flood. The city contains the mouth of the island's longest river, Río de la Plata, which drains into the Atlantic Ocean on the northern edge of the municipality. Proximity to these major water features and the flat, low terrain contribute to the flood-prone nature of the area. During tropical storm events, such as Hurricane Maria in 2017, Toa Baja experienced inundation of up to 20 feet. Changes in the global climate system are causing more intense and frequent tropical storms, making places like Toa Baja subject to irreparable damage. This NASA DEVELOP project collaborated with the Municipio Autónomo de Toa Baja, ResilientSEE, and the Massachusetts Institute of Technology Urban Risk Lab to supplement recent 2018 Federal Emergency Management Agency Hydraulic Engineering Centers-River Analysis System flood maps, which designated 63% of the area as a flood plain. The analysis provides a high-resolution interpretation of flood susceptibility using a variety of factors that collectively influence the likelihood of flooding. Sentinel-1 C-Band Synthetic Aperture Radar (C-SAR) data processed with Google Earth Engine scripting identified historical inundation and was used for validation purposes. Socioeconomic factors were combined with the inundation layer producing a final risk output. These outputs will improve public understanding of exposure to flood risk in Toa Baja and provide scientific evidence for flood mitigation advocacy.

Keywords: Landsat, NASA, ESA, Google Earth Engine, ArcGIS Pro, SAR, flood risk, flood susceptibility, tropical storms

2. Introduction

2.1 Background Information

Flood events cause an average of 40 billion dollars in infrastructure damage per year worldwide (Organisation for Economic Co-operation and Development, 2016). The hurricane season of 2017 was the costliest in United States history, with Hurricane Maria causing 103 billion dollars in economic losses to Puerto Rico alone (Halverson, 2018). In the Municipality of Toa Baja (*Figure 1*), nearly 14,000 homes were flooded, resulting in 1.3 billion dollars in damage. The northeast coast of Puerto Rico floods frequently due to heavy rainfall, storm surge inundations, and its unique topography (López-Marrero & Yarnal, 2010). Toa Baja, referred to by locals as the "Underwater City," has more than 60% of its land designated as floodplain (Federal Emergency Management Agency, 2009). Tropical storms, exacerbated by warming oceans and sea-level rise, are a growing concern to citizens in this municipality.

Gauging relative flood susceptibility involves the analysis of various criteria that influence the likelihood of flooding. Susceptibility refers to the relative likelihood of flooding for any given location in the study area. Flood vulnerability looks only at socioeconomic factors such as population and building density. The combination of flood susceptibility and vulnerability is flood risk. Gauging relative flood risk gives the municipality a better picture of the most vulnerable and susceptible areas. Methods used to analyze susceptibility and risk involved multi-criterion evaluation- criterion, where criteria are weighted using the analytic hierarchy process (AHP). In the realm of natural hazard modeling, the AHP is one of the most commonly used methods of ranking the influence of criteria (Tehrany, Pradhan, & Jebur, 2014). The AHP is an easy to use multi-criteria weight estimation method of assigning numerical values to abstract concepts (Saaty, 1988; Zou et al., 2013). Nine criteria were selected as flood-influencing factors in our analysis based on previous literature and available data (Kia et al., 2012; Roopnarine et al., 2018; Tehrany et al., 2014). To validate our analysis, we used the European Space Agency's (ESA) Sentinel-1 & 2 and NASA Landsat 5 & 7 satellite imagery to map actual past inundation using Google Earth Engine. Our analysis builds upon existing Federal Emergency Management Agency (FEMA) flood risk maps by utilizing Earth observations and providing a finer resolution than the large vector polygons which they used to define Toa Baja flood risk. Our results were compared against actual inundation for validation purposes.

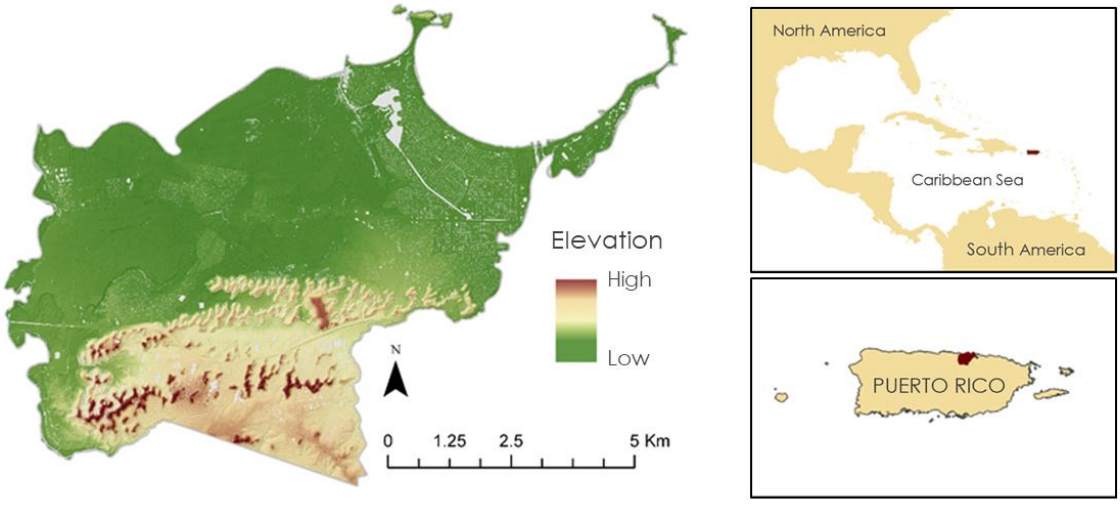

Figure 1. The study area of this project is the Municipality of Toa Baja on the northern coast of Puerto Rico. Toa Baja is located just outside of San Juan and is known as *"La Ciudad Bajo Aguas"* or "the underwater city" due to its propensity to flooding from its unique geography and the island's location in "hurricane alley."

2.2 Project Partners & Objectives

This project partnered with the Municipio Autónomo de Toa Baja, ResilientSEE, and the Massachusetts Institute of Technology (MIT) Urban Risk Lab. The Municipio Autónomo de Toa Baja is a local government entity. The Municipality employs professionals to provide the Mayor with available data and analysis for infrastructure and emergency planning. Prior to our study, the municipality utilized official 2005 FEMA Flood Insurance Rate Maps (FIRM) and the most recent 2018 Hydrologic Engineering Center's River Analysis System (HEC-RAS) Puerto Rico Advisory Maps in their planning. Our additional partners were ResilientSEE a nonprofit with the mission of combining social, environmental, and economic factors to improve the quality of life and extreme weather event preparedness in Puerto Rico. Also, the MIT Urban Risk Lab collaborated with the team to provide insight on project methodology and final products.

The primary goal of this project was to create a static flood susceptibility map of the study area by combining weighted factors such as elevation, slope, and soil moisture. Additionally, a flood risk map was created by incorporating additional human-related variables to account for human flood impacts. To validate the outputs, the susceptibility and risk maps were compared against actual historical flooding that occurred during Hurricane Maria in 2017 as well as the 2018 HEC-RAS maps.

The Municipality of Toa Baja was interested in informing its residents on relative flood risk within the municipality. Previously, the only resource for the public to gauge relative flood risk for their area was the 2009 FEMA FIRM. Our analysis builds upon the 2009 measure of flood risk and made the results accessible through a Toa Baja-specific ArcGIS Online StoryMap. This simple interactive map allows residents to explore flood risk, susceptibility, and contributing factors with ease. This project fills the need for data-based products to inform government and public decision making.

3. Methodology

Esri ArcGIS Pro software was used to process datasets and to create flood susceptibility, vulnerability, and flood risk maps (Roopnarine et al., 2018). We weighted and combined nine different flood factor raster datasets to assess the overall flood susceptibility (*Figure 2*). The actual occurrence of inundation was used to validate our measure of flood susceptibility. Synthetic aperture radar (SAR) data from ESA's Sentinel-1, made available through Google Earth Engine (GEE), were used to map historical flood inundation that occurred during hurricane Maria in 2017, Hurricane Irma in 2017, and flood events on February 24, 2020 and October 10th, 2017 for validation of the susceptibility map.

GEE is advantageous because large datasets can be stored, processed, and analyzed on this cloud-computing platform. Utilizing GEE eliminated the laborious data download process associated with traditional remote sensing flood analysis (DeVires, et al., 2020). Use of Landsat data was also explored for flood detection, but did not yield usable imagery due to clouds and capture timing. SAR proved to be the ideal satellite imagery for detecting inundation in cloudy conditions, while optical sensors proved insufficient (Shen et al., 2019).

3.1 Data Acquisition

This analysis involved Earth observation imagery (see Appendix, Table A1), ancillary raster datasets (see Appendix, Table A2), and ancillary vector datasets (see Appendix, Table A3). Earth observations were utilized to measure vegetation and flood detection. GEE Application Programming Interface (API) was used to calculate NDVI for input in the susceptibility analysis and to map inundated areas for validation. This was completed using code from DeVires et al., 2020 and the United Nations Office for Outer Space Affairs Knowledge Portal. To improve the interpretability of our final flood risk output, the census tracts from the American Community Survey 2017 were used to summarize risk using the mode pixel value. The shapefile was derived from ArcGIS Online (see Appendix, Table A3).

3.1.1 Flood Susceptibility Criteria

Nine different criteria were weighted based on their contribution to a flood event and combined to create the flood susceptibility map (*Figure 2*). The landcover variable accounts for the influence of varying surface types on flood susceptibility. Forested areas are less likely to experience flooding than urban landscapes because of the difference in groundcover permeability. The Normalized Difference Vegetation Index (NDVI) is a measure of relative vegetation health. This parameter accounts for the associated influence of plant root networks on rain runoff. Elevation accounts for the influence of gravity on the movement of water in the landscape. The slope parameter factors in where water will accumulate based on the land gradient. The topographic wetness index (TWI) models runoff based on elevation. TWI adds an additional layer of robustness as opposed to factoring only slope and elevation and is described as an "indicator of the effect of local topography on runoff flow direction and accumulation" (Ballerine, 2017). The height above the nearest drainage (HAND) is an approximate measure of the vertical height of a given pixel from the nearest flow accumulation area. This is a uniformly comparable, landscape-normalized model found to influence flood susceptibility in previous research such as Armenakis, Romero, and Usman, 2018. The saturated hydraulic conductivity (KSAT) parameter is a measure of the speed that water infiltrates soil in millimeters per second. Infiltration rates influence the amount of runoff during a rainfall event and is therefore an important factor in flood susceptibility. Storm surge hazard must also be considered, as Toa Baja is a coastal municipality, where tropical storms and hurricanes are a frequent contributor to flooding events. The last parameter considered was distance to water, which accounts for riverine floodplains in the study area.

3.1.2 Digital Elevation Model

Ancillary raster datasets included soil properties, elevation, land cover classes, and storm surge hazards, and these datasets were essential in calculating flood susceptibility, flood risk, and for validation of our results. The soil infiltration rate raster layer was downloaded from the United States Department of Agriculture Web Soil Service. Elevation data were downloaded from a National Oceanic and Atmospheric Administration (NOAA) site hosting the United States Geological Survey Lidar data. The spatial coordinate-specific tiles

were individually downloaded from their file transfer protocol site and then merged. High resolution landcover data from 2010 were provided by NOAA Office for Coastal Management. Storm surge data were retrieved from the National Hurricane Center and Central Pacific Hurricane Center website, which is also affiliated with NOAA.

3.1.3 KSAT

The KSAT variable was downloaded directly from the USDA web soil service. To download the data, first an area of interest polygon is created. Then, navigation through the 'Soil Data Explorer' and subsequent 'Soil Properties and Qualities' tab is necessary. Once there, the saturated hydraulic conductivity (KSAT) data was downloaded from the 'Soil Physical Properties' menu, at a depth of 10cm.

3.1.3 Storm Surge

Storm Surge was adapted from the Sea, Lake, and Overland Surges from Hurricanes (SLOSH) model from the National Weather Service. The SLOSH model takes into account a specific shoreline and applies physics equations factoring the wind field driving the storm surge. Landcover was acquired from the NOAA Office for Coastal Management and was used without alteration.

3.1.5 Vector datasets

Hydrological features vector data were sourced from the Puerto Rican government website, provided by the Centro de Recaudación de Ingresos Municipales, Oficina de Gerencia y Presupuesto. The building footprints were provided by crowdsourced data entry from OpenStreetMap and downloaded for our specific area through the GeoFabrik website. The 2018 FEMA Hydraulic Engineering Center's River Analysis System (HEC-RAS) flood risk data were downloaded directly from the Toa Baja Municipality website and were used to validate our final flood susceptibility model.

3.1.6 Flood Vulnerability Criteria and Mapping

Three different criteria were used to determine vulnerability to flooding. Population density and building density layers were used as measures of vulnerability, as determined by previous studies (Roopnarine, 2018). Our team sourced the building density data from OpenStreetMap and population data from World Pop. In addition to the aforementioned data layers, an informal settlements layer, which was provided by the Toa Baja Municipality, was also included. Such settlements are vulnerable to inclement weather due to the fragility of their socioeconomic status and housing conditions. Homes built in informal settlements may be more vulnerable to damage in the case of extreme weather events. These three datasets were combined in ArcGIS Pro creating a single vulnerability raster layer.

3.2 Data Processing

Various datasets were combined using the raster calculator tool in Esri ArcGIS Pro 2.3.0 to create the flood susceptibility, vulnerability, and risk maps. Linear combination involved harmonizing all inputs into the same scale, projecting to the NAD83 NSRS 2007 coordinate system, and calculating weights using the analytical hierarchy process (Saaty, 1994). The weighted combination with a raster calculator is also known as a weighted linear combination (Pourghasemi, Pradhan, & Gokceoglu, 2012).

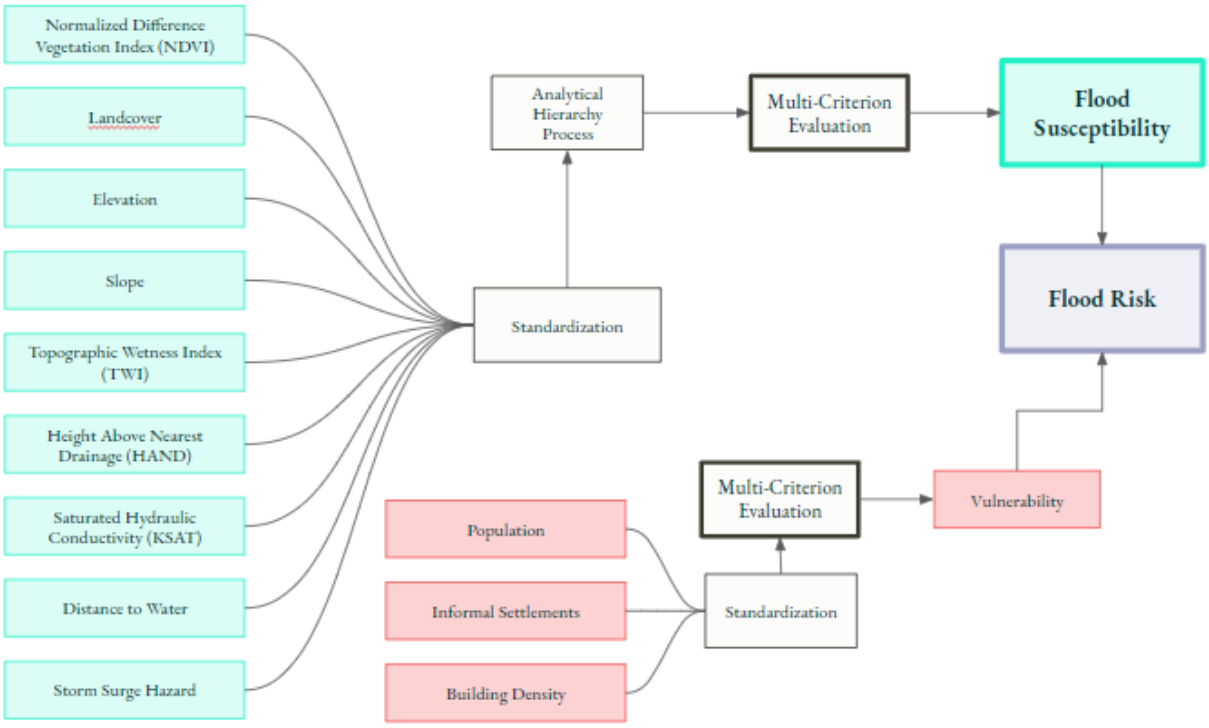

Figure 2. Flowchart of the process involved in creating the flood susceptibility and flood risk.

The flood susceptibility output had three different forms, based on the weighting schemes derived from consultation with three experts who informed the weights through the AHP pairwise comparison matrix. To determine which version of the flood susceptibility output to use, we compared each with actual inundation caused by previous flood events. This was done using RStudio, via correlation between flooded pixels and flood susceptibility value, and visual comparison of the segregation of peaks in histograms which were masked to flooded and non-flooded pixels of the susceptibility outputs. The most accurate model of flood susceptibility was both the most correlated with actual inundation and had a more notable separation of histogram peaks indicating lower susceptibility values in non-flooded areas and higher susceptibility values in previously flooded areas.

3.2.1 Static Flood Susceptibility Map

Some inputs to the flood susceptibility map simply required clipping and scale standardization. Others required more processing. The following specifies the additional processing conducted. Elevation data from the NOAA coastal LiDAR scan were mosaicked into a high-resolution 1-meter digital elevation model (DEM). Distance to water, elevation and slope layers were derived using ArcGIS Pro spatial analyst tools. Elevation and slope were created using the DEM, and distance to water was derived from the vector layer Toa Baja rivers.

The NDVI factor was produced in GEE. Sentinel-2 MSI images were filtered to the dates 09/01/2019 through 10/31/2019. A GEE script was developed to derive the median pixel value and mask clouds, eliminating a potentially cumbersome step in other scripting environments. From the DEM, we calculated TWI within ArcGIS Pro using multiple tools from the spatial analyst toolbox as outlined in *Figure 3*. The tools included flow direction, flow accumulation, slope, and raster algebra expressions all based upon the original DEM (Hojati & Mokarram, 2016).

The elevation dataset was also used to derive height above nearest drainage (HAND) criterion. The HAND was calculated using a publicly available premade ArcGIS tool which involves the creation of flow direction, flow accumulation, and other parameters to derive the final output (Rahmati, 2018). The tool's script was originally created for use in ArcGIS desktop, which we adapted for functionalization in ArcGIS Pro using Python.

3.2.2 Analytical Hierarchy Process

After the criteria were selected, they were arranged in a hierarchy based on the previously established methods widely available in literature (Roopnarine et al. 2018; Kazakis, Kougias, & Patsialis 2015; Samanta, Kumar Pal & Palsamanta, 2018; Elsheikh, Ouerghi, & Elhag, 2015; Tehrany et al., 2014a, 2014b). To determine the relative weight of each factor in the susceptibility analysis we used the Analytical Hierarchy Process (AHP), which is described as "a multi-objective, multi-criteria decision-making approach" by Yalcin (2008). This required experts to complete a pairwise comparison matrix, which assigns relative weights to all nine parameters (see Appendix, Table A4).

Three experts completed the pairwise comparison matrix to inform the AHP. The three resulting weighting schemes were applied to the susceptibility factors for the weighted linear combination. This resulted in three different versions of flood susceptibility, which were each then compared against a consolidated inundation footprint of four different flood events. The flood inundation was detected using SAR data in GEE. The APH model that aligned the best with actual inundation was used as our final flood susceptibility result. Compatibility was measured in R through basic statistical correlation and pixel histogram comparison.

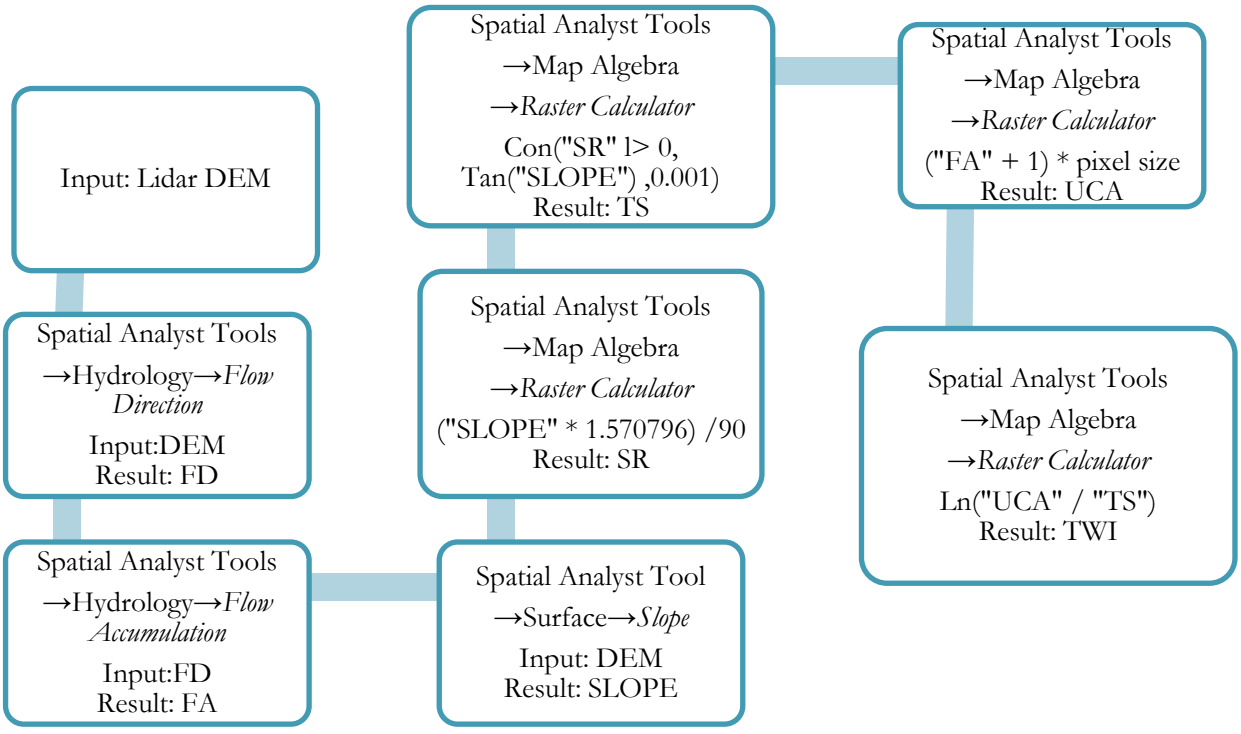

Figure 3. Flow chart illustrating the creation of TWI with ArcGIS Pro 2.3.0 spatial analyst tools and raster algebra expressions.

3.3 Data Analysis

Determining which flood susceptibility model to use as our final, of the three different weighing schemes, was done via comparison with actual inundation detected with GEE. Correlation was the intuitive method of statistically assessing which dataset correlated best with inundation. When this did not produce compelling

enough evidence for selection (see Appendix, Table A5), we additionally assessed the histogram peaks of susceptibility pixels masked for both flooded and non-flooded areas (see Appendix, *Figure B1*). The most accurate model was determined to be 'Option C' which is highlighted in yellow in the corresponding table and figure referenced above.

The team used weighting from 'Option C' to create the final vulnerability and susceptibility layers. The vulnerability layer combined with the weighted susceptibility layer form the final static flood risk output (*Figure 4*). This bivariate method of depicting flood risk was chosen because it still preserves both measures of susceptibility and risk while allowing the additional measure of cumulation. The three layers are all continuous raster datasets and can be used as separate measures to inform decision-making. The risk dataset, being of most interest to our partners, was averaged by regions within Toa Baja for a measure of relative flood risk as a zonal summarized value. To improve the interpretability of the final flood risk output, the mode pixel value was assigned to the corresponding American Community Survey census tract (*Figure 5*). This was to makes findings more usable operationally.

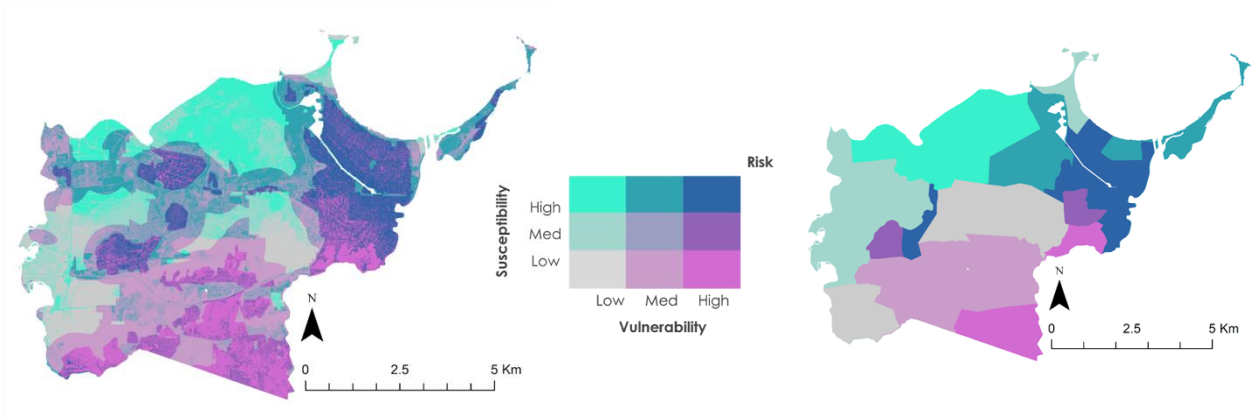

Figure 4 and Figure 5. On the left is the final risk map, highlighting the intersection of vulnerability and susceptibility throughout Toa Baja (*Figure 4*). On the right is a risk map summarized by census tract (*Figure 5*). Both maps were generated using 'Option C' weighting.

4. Results & Discussion

4.1 Analysis of Results

Our risk map shows nine levels of varying risk. The bivariate legend (*Figure 4*) illustrates high susceptibility and low vulnerability in light blue. These show areas where flooding is likely, but there are little to no vulnerable populations. The light blue in our map aligns with a northern area designated as wetlands. Magenta within the map delineates high vulnerability areas with low susceptibility. This shows us where people are living, yet are not as likely to be impacted by flooding. In our case, the magenta is clustered around the foothills of Toa Baja, where elevation and distance from the coast reduce the susceptibility to flooding. The convalescence of high susceptibility and high vulnerability is delineated in navy blue. These areas include a high population density located where floods are more likely to occur.

Because our parameters informing vulnerability were limited, which is discussed in the 'Limitations' section, it is also useful to examine flood susceptibility alone (see Appendix, *Figure B2*). The flood susceptibility analysis values were summarized by zones defined by cardinal regions; these regions were defined and provided by the Toa Baja Municipality. The most notable finding is that the northern region was found to be nearly 50% highly susceptible to flooding (see Appendix, *Figure B3*). Highly susceptible was defined here as being from 3.66-5 on the scale of 1-5. Finer summary statistics at the census tract level found some areas to be as high as 64% susceptible to flooding (see Appendix, *Figure B4*).

4.2 Validation

To validate our flood susceptibility map, we compared the result with the 2018 HEC-RAS FEMA Flood Advisory Maps (*Figure 6*), which are the most updated maps that the municipality utilizes as a reference. The HEC-RAS dataset was developed in coordination with FEMA in 2018 following Hurricane Maria. This dataset increased the proportion of estimated flood zone in Toa Baja from 48% in previous FEMA estimates to 63%. These maps establish different zones to characterize flood hazards. We added an "outside flood zone" (OFZ) class to delimit zones in Toa Baja outside the zone polygons established by FEMA.

Table 2

Percent pixel agreement between HEC-RAS Advisory Maps and flood susceptibility map.

		FLOOD SUSCEPTIBILITY		
		High	**Moderate**	**Low**
HEC-RAS ZONE	**A - floodway**	89.42%	65.61%	20.95%
	AE - coastal A zone	2.92%	2.07%	0.46%
	VE - flood zone	0.67%	0.63%	0.34%
	X - 0.2% annual flood	3.03%	2.74%	1.81%
	OFZ - outside flood zone	3.94%	28.93%	76.43%

The results show spatial coherence between HEC-RAS Maps and our flood susceptibility map. To validate our model, we divided it into three classifications: High, Moderate, and Low. We compared the percentage in each category with the FEMA zones (Table 2). Zone A contains 89.42% of the High susceptibility values. This represents the floodway with a 1% annual chance flood. However, Zone A also contains the most Moderate susceptibility values at 65.61%. Zone X, which represents a 0.02% annual chance of flooding, contains 3.03% of the high susceptibility values. The OFZ zone, which represents areas outside of FEMA's floodplain designation, is primarily dominated by low and medium values at 76.43% and 28.93% respectively. This indicates accuracy in our map. Even so, we must emphasize that 20.95% of the Low susceptibility values are within Zone A, which indicates uncertainty in this study, as we would expect a small percentage of Low susceptibility values in an ideal agreement.

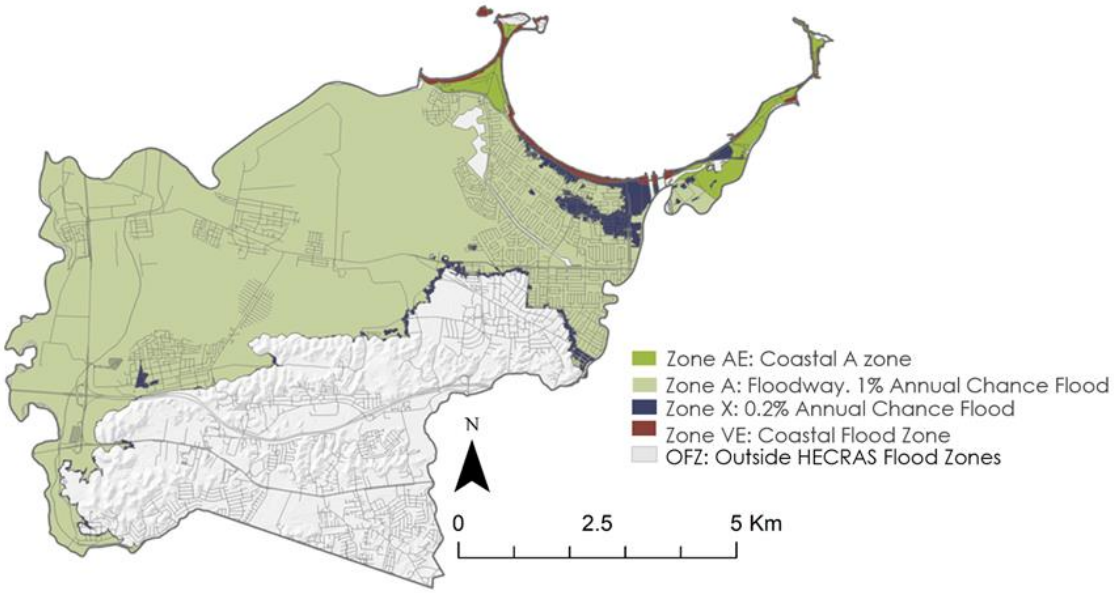

Figure 6. 2018 HEC-RAS FEMA Flood Advisory Maps.

4.3 Limitations

SAR imagery has been known to collect false positive flooding from building shadows in urban areas, and Toa Baja has multiple urban areas where we attempted to detect flooding. These false positives may have appeared in our flood inundation detection through GEE, but we were unable to measure these potential errors without *in situ* inundation data. Additionally, this project created a static flood susceptibility map using multiple assumptions to accommodate our study area and partners' needs. Storm surge and riverine flooding are two types of flooding accounted for in our analysis, but ideally, they should be assessed separately. Our weights were assigned based on expert knowledge after we consulted three scientists. There is inherent error in these weight assignments, and our experts did not agree on any particular weighting scheme. Due to limitations in data availability, this study does not account for age or income in our measure of vulnerability. However, the team recognizes these are-social groups that will likely be more vulnerable during times of disaster. Recent granular demographic information is necessary to be able to incorporate these variables into raster-based analyses.

4.4 Future Work

Our study used Sentinel-1 C-SAR data to detect past flooding in Puerto Rico, given that NASA has no current SAR sensor. Future studies can use our project as a template for the NASA-ISRO SAR mission, which is scheduled to launch in 2021. Our team attempted to incorporate MODIS observation imagery, but the spatial resolution of 250-meters was too coarse for our small study area. Additionally, the short ten-week completion window for our project limited the validation capabilities. Incorporating soil moisture, rainfall data, man-made hydrological features, and previous storm flood depth measures into a flood risk assessment can be done in the future to improve upon our analysis.

In terms of methodology, a factor-weighting method could be incorporated by making a covariance matrix with each layer and a target variable (for example, a flood raster). This produces a rough estimate of how each variable contributes to the flood raster. Due to the limited time, we-were unable to utilize this approach, yet it remains a feasible quantitative methodology for future work.

5. Conclusions

The Municipality of Toa Baja experienced devastating flooding during Hurricane Maria, and their leadership aims to prepare for future flooding events their residents may face. Their main concern is prioritizing the

distribution of limited resources to their most at-risk residents. Our project exemplifies how the interpretation of flood risk can be improved through the use of Earth observations. Through our analysis, we found the east region of Toa Baja is most at risk for flooding, due to the high susceptibility to flooding in tandem with a high density of population, buildings, and informal settlements. However, we found that the north region is most susceptible to flooding given its proximity to the coast and the preponderance of wetlands in this region. The south is the least at risk in our model, mainly because of the distance from the coast and the elevation provided by foothills. Our risk map also shows there are smaller "at risk" areas all around the municipality. This granular analysis provides our partners with an improved understanding of where they can allocate resources in times of an emergency. Additionally, these results are presented in an accessible platform to easily inform the public about their risk and susceptibility to flooding.

6. Acknowledgments

The Toa Baja Disasters team would like to thank our science advisors Dr. Kenton Ross, Dr. Venkat Lakshmi, and our Fellow Sydney Neugebauer for their guidance throughout the project. We would also like to thank our partners at the Municipality of Toa Baja, ResilientSEE, and MIT Urban Risk Lab for their clear communication and enthusiastic participation. Additionally, we'd like to thank Dr. John Bolten, Dr. Marangelly Cordero-Fuentes and Perry Oddo for their valuable contributions to the project.

This material contains modified Copernicus Sentinel data (2019), processed by ESA.
Any opinions, findings, and conclusions or recommendations expressed in this material are those of the author(s) and do not necessarily reflect the views of the National Aeronautics and Space Administration.
This material is based upon work supported by NASA through contract NNL16AA05C

7. Glossary

GEE - Google Earth Engine
FEMA - Federal Emergency Management Agency
NDVI - Normalized Difference Vegetation Index
TWI - Topographic Wetness Index
HAND - Height Above the Nearest Drainage
GIS - Geographic Information Systems
KSAT - Saturated Hydraulic Conductivity
HEC-RAS - Hydrologic Engineering Center's River Analysis System
NISAR - NASA-Indian Space Research Organization (ISRO) SAR Mission
PCRaster - Open source software for environmental modeling.
SoilGrids - Publicly available global soil properties data maps.
NOAA - National Oceanic and Atmospheric Administration

8. References

Armenakis, C., Romero, R. D., & Usman, T. (2018). Flood risk mapping using GIS and Multi-Criteria Analysis: A Greater Toronto Area case study. *Geosciences*, *275*. doi:10.3390/geosciences8080275

Ballerine, C. (2017). Topographic Wetness Index urban flooding awareness act action support. Illinois State Water Survey. https://www.isws.illinois.edu/pubdoc/CR/ISWSCR2017-02.pdf

DeVries, B., Huang, C., Armston, J., Huang, W., Jones, J., & Lang, M. (2020). Rapid and robust monitoring of flood events using Sentinel-1 and Landsat data on Google Earth Engine. *Remote Sensing of Environment, 240*, 1-14. https://doi.org/10.1016/j.rse.2020.111664

Elsheikh, R.F.A., Ouerghi, S. & Elhag, A.R. (2015). Flood Risk Map Based on GIS, and Multi Criteria Techniques (Case Study Terengganu Malaysia). *Journal of Geographic Information System,* 7, 348-357. doi: 10.4236/jgis.2015.74027

Federal Emergency Management Agency (FEMA) Flood Map Service Center and National Flood Insurance Program. (11/2009). FEMA Flood Insurance Map (FIRM), FEMA Flood Map Service Center, accessed 24 February 2020. https://msc.fema.gov/portal/search?AddressQuery=toa%20baja#searchresultsanchor

Halverson, J. B. (2018). The costliest hurricane season in US history. *Weatherwise*, *71*(2), 20-27. https://doi.org/10.1080/00431672.2018.1416862

Hojati, M., & Mokarram, M. (2016). Determination of a Topographic Wetness Index using high resolution digital elevation models. *European Journal of Geography*, *7*(4), 41-52. Retrieved from: http://www.eurogeographyjournal.eu/articles/4.%20DETERMINATION%20OF%20A%20TOPOGRAPHIC%20WETNESS%20INDEX%20USING%20HIGH%20RESOLUTION%20DIGITAL%20ELEVATION%20MODELS.pdf

In Detail: Recommended Practice: Flood Mapping and Damage Assessment using Sentinel-1 SAR data in Google Earth Engine. (2019). Retrieved from: http://www.un-spider.org/advisory-support/recommended-practices/recommended-practice-google-earth-engine-flood-mapping/in-detail

Kazakis, N., Kougias, I., & Patsialis T. (2015). Assessment of flood hazard areas at a regional scale using an index-based approach and Analytical Hierarchy Process: Application in Rhodope-Evros region, Greece. *Science of the Total Environment,* 538, 555-563. Retrieved from: http://dx.doi.org/10.1016/j.scitotenv.2015.08.055

Kia, M., Pirasteh, S., Pradhan, B., Mahmud, A. R., Sulaiman, W. N. A., & Moradi, A. (2012). An artificial neural network model for flood simulation using GIS: Johor River Basin, Malaysia. *Environmental Earth Sciences, 67*, 251-264. https://doi.org/10.1007/s12665-011-1504-z

López-Marrero, T., & Yarnal, B. (2010). Putting adaptive capacity into the context of people's lives: A case study of two flood-prone communities in Puerto Rico. *Natural Hazards*, *52*, 277-297. Retrieved from: https://doi.org/10.1007/s11069-009-9370-7

Organisation for Economic Co-operation and Development (OECD) (2016). *Financial Management of Flood Risk*. OECD Publishing, Paris. http://dx.doi.org/10.1787/9789264257689-en https://read.oecd-ilibrary.org/finance-and-investment/financial-management-of-flood-risk_9789264257689-en#page14 date accessed 2/20/20

Pourghasemi, H. R., Pradhan, B., & Gokceoglu, C. (2012). Application of fuzzy logic and analytical hierarchy process (AHP) to landslide susceptibility mapping at Haraz watershed, Iran. *Natural hazards*, *63*(2), 965-996. Retrieved from: https://link.springer.com/article/10.1007/s11069-012-0217-2?shared-article-renderer

Rahmati, O., Samadi, M., Kornejady, A., & Melesse, A. (2018) Development of an automated GIS tool for reproducing the HAND model. *Environmental Modeling and Software*, 102, 1-12. Retrieved from: https://www.sciencedirect.com/science/article/pii/S1364815217310034

Roopnarine, R., Opadeyi, J., Eudoxie, G., Thong, G., & Edwards, E. (2018). GIS-based flood susceptibility and risk mapping Trinidad using weight factor modeling. *Caribbean Journal of Earth Science, 49*, 1-9. Geological Society of Jamaica. Retrieved from: https://www.researchgate.net/publication/326925603_GIS-based_Flood_Susceptibility_and_Risk_Mapping_Trinidad_Using_Weight_Factor_Modeling

Saaty, T. L. (1988). What is the Analytic Hierarchy Process? *Mathematical Models for Decision Support.* In: Mitra G., Greenberg H.J., Lootsma F.A., Rijkaert M.J., Zimmermann H.J. (eds) NATO ASI Series (Series F: Computer and Systems Sciences), 48, 109-121. Springer, Berlin, Heidelberg.

Saaty, T. L. (1994). How to make a decision: the analytic hierarchy process. *European journal of operational research*, *48*(1), 9-26. Retrieved from: https://pubsonline.informs.org/doi/abs/10.1287/inte.24.6.19

Samanta, S., Kumar Pal, D., & Palsamanta B. (2018). Flood susceptibility analysis through remote sensing, GIS and frequency ratio model. *Applied Water Science, 8, 66*. https://doi.org/10.1007/s13201-018-0710-1

Shen, X., Wang, D., Mao, K., Anagnostou, E., & Hong, Y. (2019). Inundation extent mapping by Synthetic Aperture Radar: A Review. *Remote Sensing*, *11*, 879. doi:10.3390/rs11070879

Tehrany, M. S., Pradhan, B., & Jebur, M. N. (2014a). Flood susceptibility mapping using a novel ensemble weights-of-evidence and support vector machine models in GIS. *Journal of Hydrology,* 512, 332-343. Retrieved from: http://dx.doi.org/10.1016/j.jhydrol.2014.03.008.

Tehrany M. S., Lee, M.-J., Pradhan, B., Jebur M. N., & Lee, S. (2014b). Flood susceptibility mapping using integrated bivariate and multivariate statistical models. *Environmental Earth Sciences, 72,* 4001-4015. Retrieved from doi: 10.1007/s12665-014-3289-3

Tehrany, M., Pradhan, B., & Jyalcebur, M. (2014). Flood susceptibility mapping using a novel ensemble weights-of-evidence and support vector machine models in ArcGIS. *Journal of Hydrology*, *512*, 332-343. doi: 10.7717/peerj.7653

Yalcin, A. (2008). GIS-based landslide susceptibility mapping using analytical hierarchy process and bivariate statistics in Ardesen (Turkey): Comparisons of results and confirmations. *Catena, 72*, 1-12. Retrieved from: https://doi.org/10.1016/j.catena.2007.01.003

Zou, Q., Zhou J., Zhou C., Song L., & Guo J. (2013). Comprehensive flood risk assessment based on set pair analysis-variable fuzzy sets model and fuzzy AHP. *Stochastic Environmental Research and Risk Assessment, 27*, 525-446. Retrived from: https://www.tib.eu/en/search/id/BLSE%3ARN325266579/Comprehensive-flood-risk-assessment-based-on-set/

9. Appendices

Appendix A

Table A1

Earth observation imagery sources used for project.

Platform & Sensor	Parameter	Use
Landsat 7 Enhanced Thematic Mapper (ETM+)	Inundation	Landsat 7 ETM+ imagery was ingested at 30 m resolution into the interactive flood mapping tool to map recent flood events.
Landsat 5 Thematic Mapper (TM)	Inundation	Landsat 5 TM data were ingested at 30 m resolution into the interactive flood mapping tool to map recent flood events.
Copernicus Sentinel-2 Multispectral Instrument (MSI)	NDVI	Copernicus Sentinel-2 MSI imagery was used to calculate the Normalized Difference Vegetation Index (NDVI) for the integration with the static susceptibility map.
Copernicus Sentinel-1 C-Synthetic Aperture Radar (SAR)	Inundation	Copernicus Sentinel-1 SAR data were used to map historical flood extent and were used to map past flood events, which were later used for validation of our model.

Table A2

List of ancillary raster datasets.

Dataset	Date Used	Use
United States Department of Agriculture Web Soil Service	2017	A Saturated Hydraulic Conductivity Layer was used to represent soil infiltration rate
United States Geological Survey (USGS) NOAA Coastal Lidar Scan Digital Elevation Model (1 m resolution)	2015	We used the USGS LiDAR DEM to calculate TWI, HAND, slope, and elevation.
NOAA Landcover	2010	We used the NOAA Coastal Change Analysis Program high-resolution 1-meter landcover from 2010 in the flood risk and susceptibility maps.
National Hurricane Center and Central Pacific Hurricane Center	2018	We used the storm surge hazard measure to account for inundation intensity resulting from coastal surge in the flood susceptibility model.

Table A3

Ancillary Vector Datasets

Dataset	Date Used	Use
Hydrography Revision from Centro de Recaudación de Ingresos Municipales (CRIM) Basemap, Puerto Rico	2001 to 2004	Calculation of distance from the water input layer for flood susceptibility analysis.
OpenStreetMap - Geofabrik	2020	Building footprints were used to create density variables for flood risk analysis.
Hydrologic Engineering Center's River Analysis System (HEC-RAS) Puerto Rico Advisory Maps	2018	These maps validated our flood susceptibility outputs.

American Community Survey	2017	Shapefile used to summarize final flood risk output

Table A4
Insert a Description here

Parameters	**Weights**		
	S1	**S2**	**S3**
Elevation	0.19	0.25	0.12
Slope	0.10	0.26	0.08
Landcover	0.03	0.16	0.04
NDVI	0.03	0.05	0.02
Storm Surge	0.31	0.11	0.23
Distance to water	0.07	0.08	0.17
Height above nearest drainage (HAND)	0.19	0.04	0.23
Topographic Wetness Index (TWI)	0.06	0.04	0.10
Saturated Hydraulic Conductivity (KSAT)	0.03	0.02	0.01

Table A5
Correlation analysis results.

	MARIA	**Sep. 2017**	**Oct. 2017**	**Feb. 2020**	**ALL**
Option B	0.20622	-0.1009	-0.0033	-0.0313	0.07252
Option C	0.19978	-0.061	0.00429	-0.0098	0.09837
Option A	0.21194	-0.0879	-0.0031	-0.0336	0.08217

Appendix B

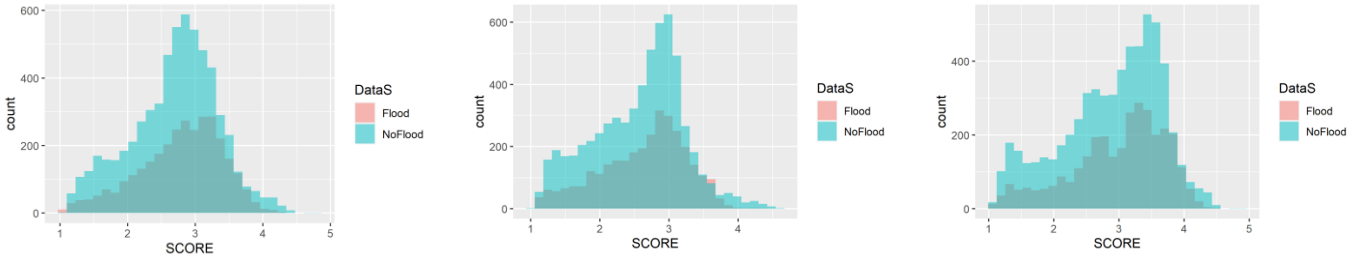

Option A Option B Option C

Figure B1. Histogram comparisons of flooded v.s. non-flooded masked flood susceptibility pixels

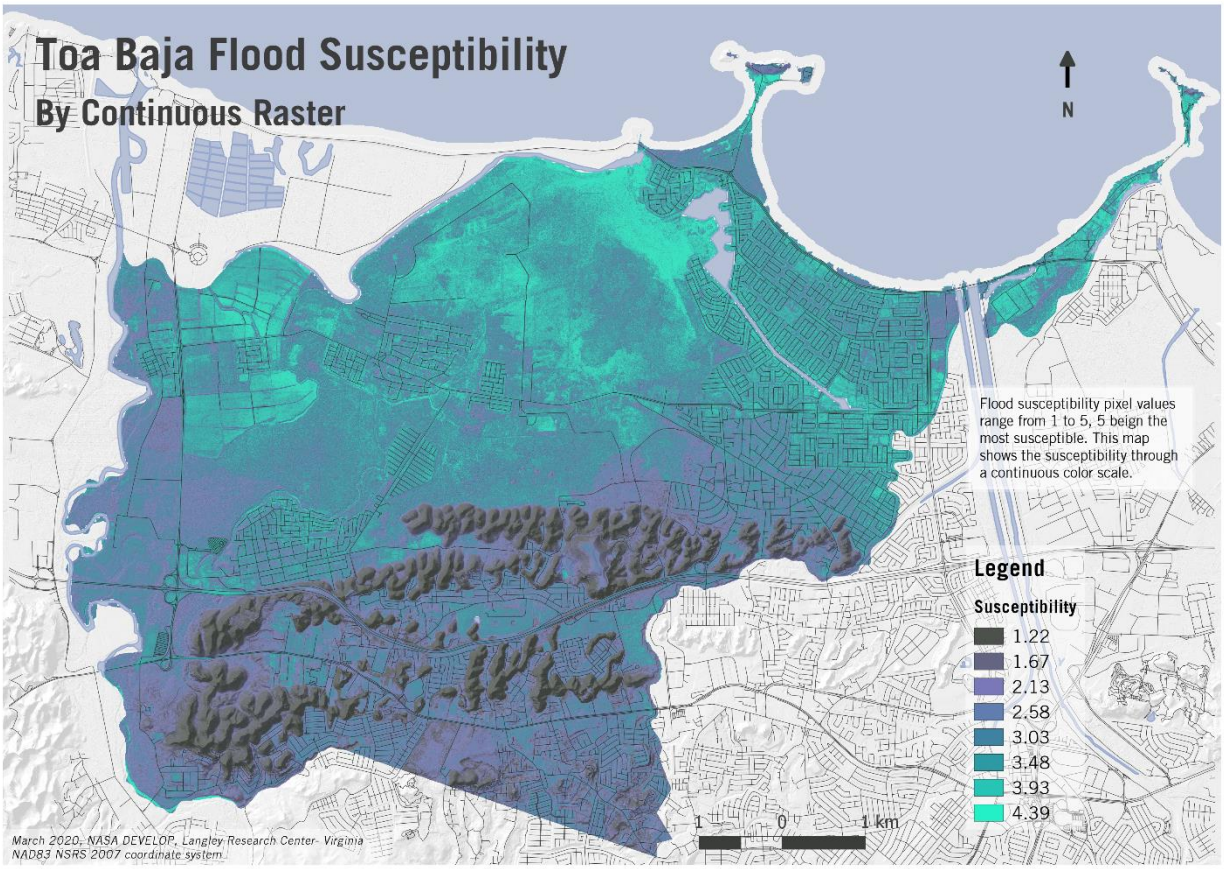

Figure B2. Flood susceptibility map.

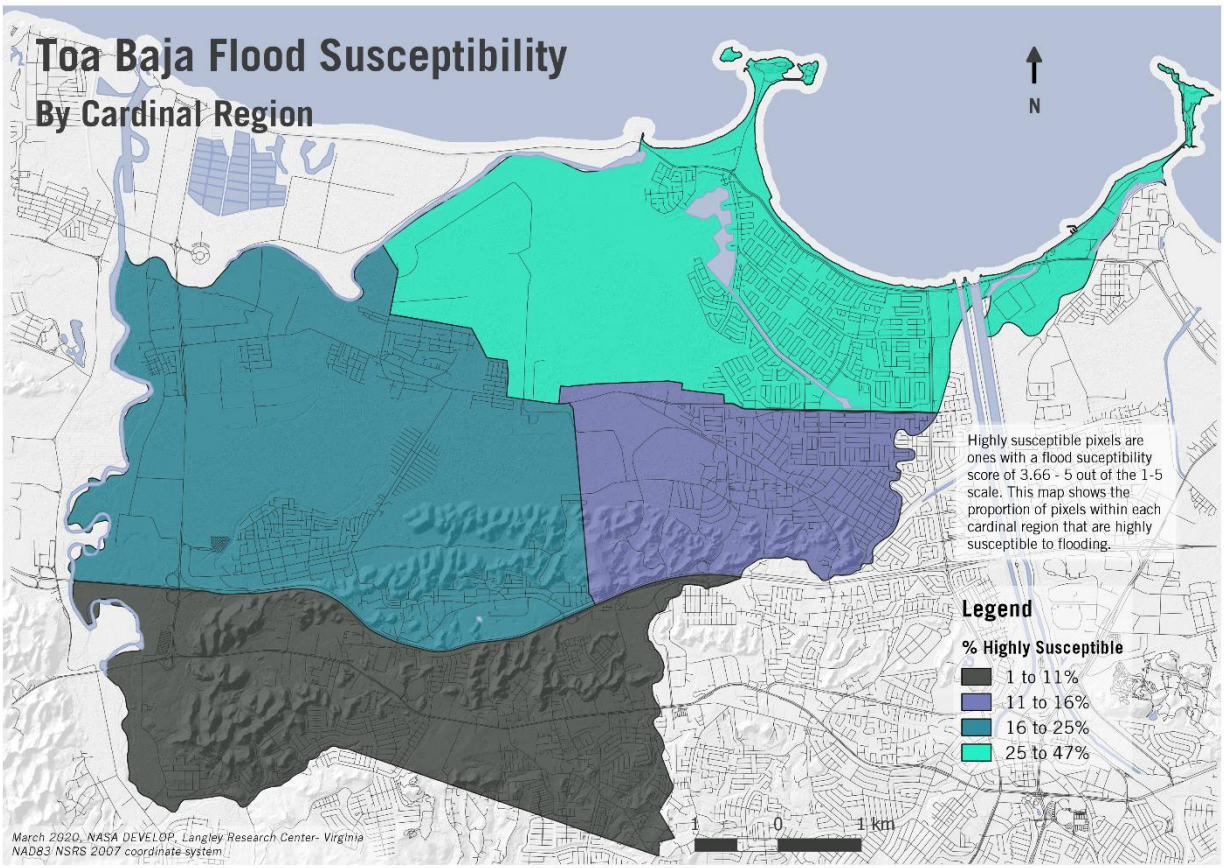

Figure B3. High flood susceptibility by cardinal zone.

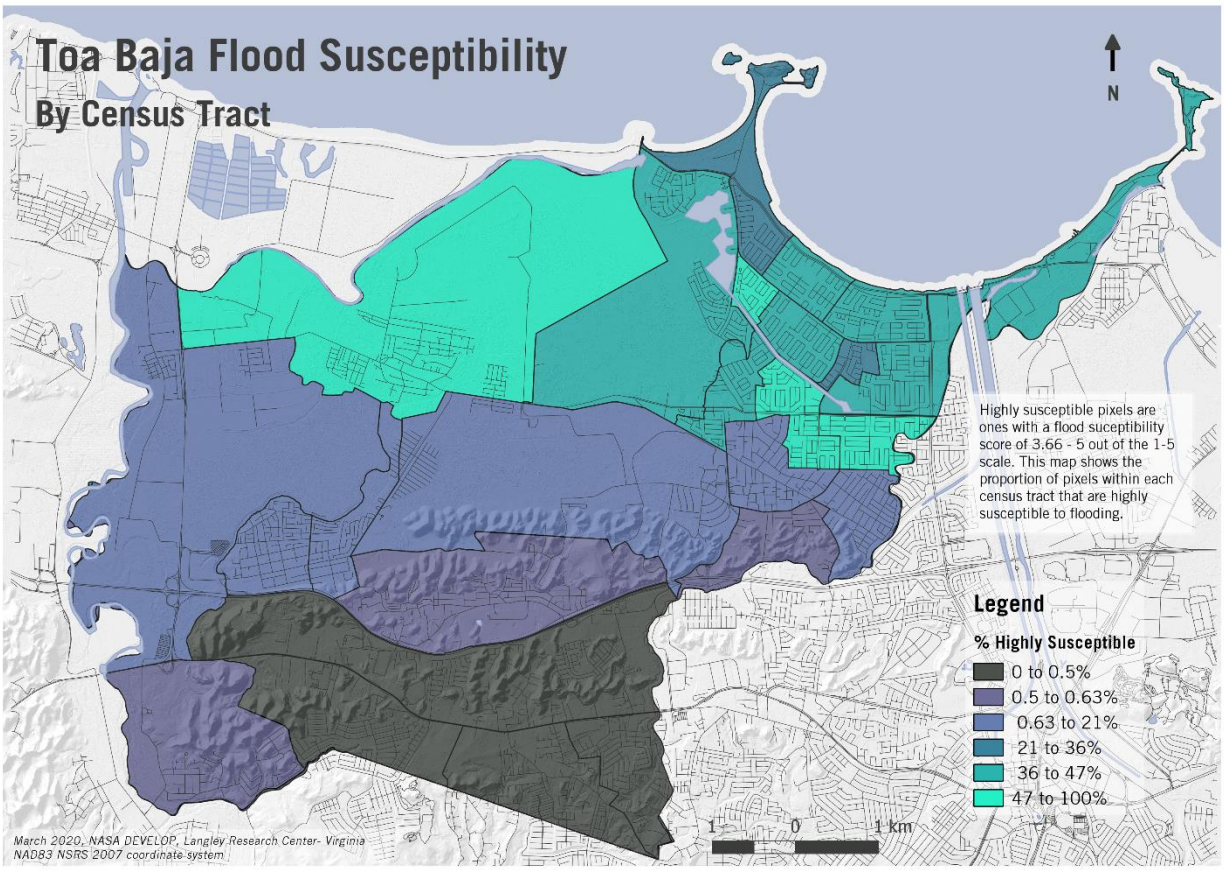

Figure B4. High flood susceptibility by census tract.